A Comparative Performance of Different Controllers for Mitigating Harmonic Distortion on 132 kV Sub-Transmission Lines Reinforced with STATCOM

M. O. Okelola[1], D. O. Aborisade[1], O. Onmoke[1], O. E. Olabode[2*]

[1]Department of Electrical Electronics and Electrical Engineering, Ladoke Akintola University of Technology Ogbomoso, Nigeria.

[2]Department of Electrical and Information Engineering, Achievers University Owo, Nigeria

ABSTRACT: Power quality issues remain one of the prominent challenges facing most of the utility grids in many third-world countries. It affects the satisfactory performance of customers' connected loads and presents significant energy loss and heightened maintenance costs to the utility company. It is on these premises that this current study investigated the performance comparison of four different controllers in the presence of a Static Synchronous Compensator (STATCOM) incorporated with 132kV sub-transmission lines. The controllers (Model Reference predictive adaptive controller (MRPAC), Genetic algorithm-based proportional integral derivative (GA-PID), genetic algorithm-based proportional integral (GA-PI), and traditional proportional integral derivative (PID) controllers), STATCOMs, and transmission lines were modelled in the Simulink environment, and the controllers were tuned appropriately to mitigate the effect of total harmonic distortion, voltage sag, and voltage swell on the sub-transmission lines. The performance comparison of these controllers was benchmarked using the rise time (RT), settling time (ST), and percentage overshoot (PO). The total harmonic distortion was 0.01, 10, 12, 10, and 2.5 for MRPAC, GA-PID, GA-PI, PID, and IEEE 519, respectively. Also, for the cases of voltage swell and voltage sag, MRPAC showed the least value of RT, ST, and PO. Conclusively, MRPAC control-based STATCOM demonstrated a superior response profile relative to the IEEE 519 standard.

KEYWORDS: Controllers, STATCOM, Sub-transmission lines, Voltage sag, Voltage swell

[Received May 13, 2025; Revised Aug. 6, 2025; Accepted Sep. 7, 2025] Print ISSN: 0189-9546 | Online ISSN: 2437-2110

I. INTRODUCTION

Power quality issues are one of the predominant problems confronting the delivery of bulk energy supply by the utility to numerous customers (Okelola and Olabode, 2018; Okelola, 2015). It occurs as any form of deviation from the normal sinusoids of currents and voltages at the rated supply frequency that is delivered to the end user's premises (Okelola, 2015; Okelola and Olabode, 2018). Generally, power quality issues can be viewed as a two-edged sword problem emanating from the utility pieces of equipment such as the transformers, and motors and also from the end-users connected pieces of equipment majorly non-linear loads such as smart television, printers, energy savings refrigerators, lighting ballasts, electric washing machines, electric blenders, and personal and desktop computer among others (Okelola and Olabode, 2018; Okelola, 2018). Similarly, the approach of strengthening the existing grid infrastructures with the integration of intermittent energy sources as well as non-dispatchable renewable energy resources has also raised some serious concerns about the possibility of events of power quality (PQ) issues due to unpredictable occurrences of fluctuations in system voltage, bilateral flow of current and instability in grid frequencies (Khetarpal, and Tripathi,2020; Ajenikoko, and Olabode, 2017; Olabode *et al.,* 2024).

These fluctuations appear in the form of waveform distortions or disturbances, such as voltage sag, voltage swell, dip, spikes, transients, outages, under- and over-voltages, and voltage interruptions, among others (Okelola, 2015; Okelola and Ajenikoko, 2018). Also, harmonic distortion is equally a member of the family of PQ events; harmonics in supply current have a devastating effect on the consumer's loads (Okelola and Ajenikoko, 2018). Fundamentally, harmonic distortion renders energy supplied by the utility to the consumers highly unsafe for the user's pieces of connected equipment, shortens the equipment lifespan, causes deterioration of component insulation, and triggers false tripping of circuit breakers and their associated protective devices, among others (Arikan *et al,* 2015; Okelola *et al,* 2019). To buttress this further, several scholarly research outputs have equally established the fact that power quality issues are also responsible for quite a number of anomalous occurrences such as overheating of current carrying conductors, malfunctioning of measuring and controlling devices, amplification of zero-crossing noises, and reduction of pieces of equipment efficiency among others (Johnson and Hassan, 2015; Okelola *et al,* 2015; Liang *et al,* 2002).

The presence of PQ events in the energy supplied by the utility has no doubt raised some basic fundamental concerns given this present dispensation that is characterized by the

*Corresponding author: olabode.oe@achievers.edu.ng

doi: http://doi.org/10.63746/njtd.v22i4.3664

massive proliferation of sophisticated power electronics-based devices at the consumers' premises whose effective and efficient functioning solely rests on the quality of energy supplied by the utility (Mughal *et al,* 2022; Ajenikoko and Olabode, 2017). Furthermore, similar trends of the proliferation of power electronics-based devices like logic controllers (Programmable and non-programmable), and variable speed drives, among others, are equally seen in modern industrial processes where process automation has taken over every sector of the manufacturing processes (Yao *et al,* 2024). The widespread adoption of manufacturing process automation is probably because of its inherent advantages, such as cost reduction, precision, real-time monitoring, and improved productivity, among others (Su *et al,* 2019).

However, there could not be automation without power electronics devices, consequently, the said process automation is primarily powered by various power electronics, and power electronics-based drives are highly sensitive to the quality of energy supplied by the utility such that the event of under voltage or over-voltage renders many of these voltage sensitive devices to be inoperative and in the worst case scenario many of these devices will refuse to come onboard even when switched-on (Su *et al.,* 2019). Close attention must be paid to addressing the power quality problem on the utility grid, most especially the third-world countries, where power quality events are predominantly the order of the day (Pilawa-Podgurski, 2020; Ajenikoko *et al,* 2017). Several algorithms permeate the literature that provide the platform for feature extraction and feature classification, which are the central ideas in power quality research.

Similarly, an ample number of mitigating approaches have equally been proposed and published in open access domain, some of which include early detection and classification (Okelola, 2015; Montalvo *et al,* 2024), use of harmonic filters (Gupta *et al,* 2020), deployment of surge arrestor (Rao and Dash, 2010) and Fuzzy logic and PID controllers (Rao and Dash, 2010; Alsammak, and Mohammed, 2021) and flexible alternating current transmission system devices (Alajrash *et al,* 2024; Olabode *et al,* 2017; Olotuah *et al,* 2025). For instance, Okelola (2015) deployed a discrete wavelet transform and a support vector machine for the detection and classification of PQ events in a synthetic signal, and the proposed approach gave a good detection and classification rate of the power quality events like sag, swell, and interruption. Furthermore, the classification and detection of PQ events using root mean square and adaptive neuro-fuzzy inference systems on different electrical appliances employed at home and offices was investigated by Okelola and Olabode (2018). Their work showed that the proposed approach demonstrated a better classification accuracy relative to previous works used as the benchmark.

Similarly, Okelola (2018) presented the utilization of a short-term Fourier transform and Bayes classifier to detect and classify power quality events on real-time voltage waveform acquired from electrical domestic appliances with the aid of Fluke, a prominent power quality analyser. The outcome of their study showed better detection and classification accuracy. Also, He and Wang (2022) presented the comparative performance of different classification algorithms to detect and classify power quality events. The approach used includes the Kalman filter, an Extreme learning machine, and a hybrid of Kalman and extreme learning machine. The authors showed that the hybrid Kalman and extreme learning machine achieved greater classification accuracy compared to the independent use of the Kalman and extreme learning algorithm. Similarly, Dekhandji *et al,* (2023) adopted long short-term memory (LSTM) and recurrent neural networks (RNN) to detect and classify power quality events using multiple synthetic signals generated in a MATLAB environment.

The authors showed that the proposed approach achieved a classification accuracy of approximately 96.3674% revealing the robustness of combining the LSTM and RNN techniques. In another work published by Xi and Li (2023) deep learning (DP), lightweight convolutional neural network (CNN) hybridized with Kalman filter (KF), and continuous wavelet transform (CWT) was employed to detect and classify power quality events on real-time signals, the proposed approach achieved significant average classification accuracy of 99% in the presence of noise level of 10 Decibel. Furthermore, Singh *et al,* (2021) employed a proportionate integral derivative (PID) controller alongside STATCOM; with this proposed approach, the distorted waveforms were observed to improve comparatively to the events of voltage dip earlier noticed in uncompensated systems.

Also, Rao and Dash (2021) presented the application of PID and Fuzzy Logic Controller (FLC) alongside a unified power quality conditioner to mitigate events of power quality. The outcome of the proposed approach was compared with the traditional PID; the study outcome showed that the harmonics in the system were reduced drastically. Similarly, Liao and Milanović (2020) investigated the joint application of a dynamic voltage restorer (DVR) and distribution STATCOM (DSTATCOM) to mitigate sags, interruptions, and swells, among others. The outcome of their study showed that DVR achieved better voltage regulation while DSTATCOM provided better reactive power compensation in the system. The above review of related works showed that a large number of authors have done tangible work in the area of PQ events detection and classification using various basic home appliances. Others have attempted the utilization of synthetic signals generated from signal generators and Matlab-based signal generators. Other researchers have attempted the utilization of various signal processing algorithms for feature extraction and feature classification for early detection and classification of PQ issues.

However, little is known about the application of controllers, as the most commonly found in the reviewed pieces of literature are PID controllers and Fuzzy-logic controllers, which are adopted for classification and detection. This current study, therefore, leverages the existing work done and delves into the application of Genetically tuned controllers to mitigate events of PQ like total harmonic distortion and voltage sag/swell control on a typical 132kV sub-transmission network. The choice of these controller was largely connected to the fact that widely utilized for various industrial processes because of their ability to provide tunable parameters based on system error to achieve system stability and optimized performance. Also, these controllers are known for simplicity,

effectiveness, and robustness. The major contribution of this current study includes:

i). Comparative performance evaluation of four different controllers, MRPAC, GA-PID, GA-PI, and PID controllers on 132kV sub-transmission line reinforced with STATCOM

ii). Metrics such as the RT, ST, and PO were adopted to benchmark the performance of each control relative to the ability to minimize the effect of voltage sag, swell, and total harmonic distortion.

The remaining part of the paper was structured as follows: Section 2 discusses the materials and methods adopted, Section 3 delves into the discussion of results, and Section 4 details the conclusion of the study.

The central focus of this paper is to provide a framework that engineers, and other stakeholders can use in selecting the most preferred wireless communication technologies based on more than one criterion to implement an excellent embedded device design. Some of the technologies reviewed in this work are Bluetooth, Long-Term Evolution (LTE), Z-wave, Classic WaveLAN, Wi-Fi and Zigbee. The selection of these technologies is based on their relevance and criteria for embedded device design such as Transmission Speed (TS), Security, Transmission Range (TR), Power Usage (PU), Development Cost (DC) and Development Complexity (DCOP). The multi-criteria method used in the selection of wireless communication technologies coupled with illustrative examples, and future work are extensively discussed in this paper.

II. MATERIALS AND METHODS

A. Modelling of a static synchronous compensator

The use of power electronics for operational enhancement of power systems is a long-time practice that began as bulk power transmission via high-voltage direct current transmission. Thereafter, FACTs were introduced which include the series type, the shunt type, and the series-shunt type static (Olabode *et al,* 2017). One of the prominent members of the series type is the static compensator (STATCOM). Its inclusion on the transmission network has provided a means of compensating for reactive power inadequacy and voltage profile enhancement among other benefits (Olabode *et al,* 2017), and its schematic diagram is shown in Figure 1. It is a power electronic-based synchronous voltage generator that can act in inductive or capacitive mode depending on the need of the network, either to inject or absorb reactive power into the system (Rao and Dash 2021; Liao and Milanović, 2020).

The DC capacitor in STATCOM is used to generate a three-phase voltage which can be easily synchronized with three three-phase transmission voltages that are coupled to a power system through a coupling transformer (Olabode *et al,* 2017; Hingoran and Gyugyi, 2000). Furthermore, there is no reactive power exchange if the output voltage equals the transmission line's three-phase voltage. If this happens, STATCOM assumes a floating state, neither injecting nor absorbing reactive power (Hingoran and Gyugyi, 2000). Also, the real power exchange can be equally initiated by adjusting the phase shift between the converter output voltage and the AC system voltage (Hingoran and Gyugyi, 2000).

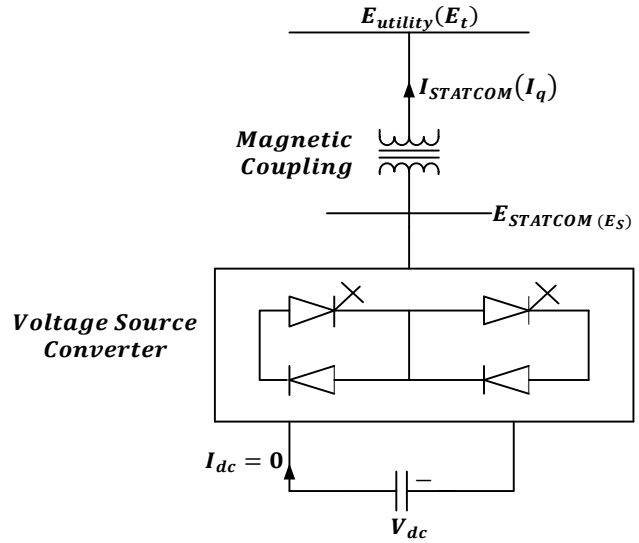

Figure 1: Schematic diagram of STATCOM (Olabode *et al.,* 2017)

To use STATCOM to absorb real power from the network, the DC system voltage from the device must lag the system alternating current voltage (Liao and Milanović, 2020; Olabode *et al,* 2017). The state-space modelling equations for a three-phase STATCOM are as given in Eqn (1a to c). The state-space equation for STATCOM is just like that of an ideal synchronous machine, which can be employed to produce a set of balanced three-phase sinusoidal voltages by adjusting the amplitude and phase angle at the nominal frequency. These sets of balance phase voltages are given thus;

$$V_{AB} = 2R(i_A - i_B) + 2L\frac{d}{dt}(i_A - i_B) + e_A - e_B \quad (1a)$$

$$V_{BC} = 2R(i_B - i_C) + 2L\frac{d}{dt}(i_B - i_C) + e_B - e_C \quad (1b)$$

$$V_{CB} = 2R(i_C - i_A) + 2L\frac{d}{dt}(i_C - i_A) + e_C - e_A \quad (1c)$$

Where; V= phase-to-phase voltage (V), i = Phase current (A), and e= STATCOM respectively for phases A, B, and C, $r_s = 2R$; line-to-line resistance of the circuit, $L_s = 2L$; line-to-line inductance of the circuit, e_A, e_B and e_C connotes sign reversal due to moving the reference point from the common connection to the ground.

Applying Kirchhof Current Law to determine the overall effect of the phase current, then the summation of all the currents in all three phases is equal to zero and is as given with Eqn (2);

$$i_A + i_B + i_C = 0 \quad (2)$$

Furthermore, the equations (1a) to (1c) above can be remodified and as described with Eqns (3) to (5), thus,

$$v_{AB} = r_a(i_A - i_B) + L_a\frac{d}{dt}(i_A - i_B) + e_{AB} \quad (3)$$

$$v_{BC} = r_a(i_A + 2i_B) + L_a\frac{d}{dt}(i_A + 2i_B) + e_{BC} \quad (4)$$

$$v_{CA} = -r_a(2i_A + i_B) - L_a\frac{d}{dt}(2i_A + i_B) + e_{CA} \quad (5)$$

Subtract Equation (3) from Equation (4) gives;

$$v_{BC} - v_{AB} = 3r_a i_B + 3L_a\frac{di_B}{dt} + e_{BC} - e_{AB} \quad (6)$$

$$\frac{di_B}{dt} = -\frac{r_a}{L_a}i_B - \frac{1}{3L_a}(v_{AB} - e_{AB}) + \frac{1}{3L_a}(v_{BC} - e_{BC}) \quad (7)$$

Similarly, subtract Equation (3) from Equation (5) yields:

$$v_{CA} - v_{AB} = -3r_a i_A - 3L_a\frac{di_A}{dt} + e_{CA} - e_{AB} \quad (8)$$

$$\frac{di_A}{dt} = -\frac{r_a}{L_a} i_A + \frac{1}{3L_a}(v_{AB} - e_{AB}) - \frac{1}{3L_a}(v_{CA} - e_{CA}) \quad (9)$$

let, $v_{AB} = v_{BC}$ and $e_{AB} = e_{BC}$ (10)

Therefore,

$$v_{CA} = -(v_{AB} + v_{BC}) = -2v_{AB} \quad (11)$$

$$e_{CA} = -(e_{AB} + e_{BC}) = -2e_{AB} \quad (12)$$

With Eqn(s) (10), (11), and (12) substituted into Eqn (9), produce Eqn (13) accordingly.

$$\frac{di_A}{dt} = -\frac{r_a}{L_a} i_A + \frac{1}{3L_a}(v_{BC} - e_{BC}) + \frac{2}{3L_a}(v_{AB} - e_{AB} \quad (13)$$

Using Equations (7) and (13), the state space representation of the AC side of the system is given as

$$\begin{bmatrix} i_A \\ i_B \end{bmatrix} = \begin{bmatrix} \frac{-r_a}{L_a} & 0 \\ 0 & \frac{-r_a}{L_a} \end{bmatrix} \begin{bmatrix} i_A \\ i_B \end{bmatrix} + \begin{bmatrix} \frac{1}{3L_a} & \frac{2}{3L_a} \\ \frac{1}{3L_a} & \frac{-1}{3L_a} \end{bmatrix} \begin{bmatrix} v_{BC} & -e_{BC} \\ v_{AB} & -e_{AB} \end{bmatrix} \quad (14)$$

The STATCOM dc side circuit equations,

$$\frac{dV_{dc}}{dt} = \frac{-1}{C_S}\left(I_{dc} + \frac{V_{dc}}{RG}\right) \quad (15)$$

The power-balance equation for the instantaneous powers at the alternating current and direct current terminals of the converter must be equal and as given thus:

$$V_{dc} I_{dc} = \frac{3}{2}(v_{BC} i_{BC} + v_{AB} i_{AB}) \quad (16)$$

$$v_{BC} = E_S \cos\theta_S = K_{CS} v_{dc} \cos\theta_S \quad (17)$$

$$v_{AB} = E_S \sin\theta_S = K_{CS} v_{dc} \sin\theta_S \quad (18)$$

Where; K_{CS} = Constant relating the AC and DC voltage of the STATCOM.

Therefore, Equation (16) becomes

$$V_{dc} I_{dc} = \frac{3}{2}(K_{CS} v_{dc} \cos\theta_S i_{BC} + K_{CS} v_{dc} \sin\theta_S i_{AB}) \quad (19)$$

where

$$I_{dc} = \frac{3}{2}(K_{CS} \cos\theta_{s\,iBC} + K_{CS} \sin\theta_S i_{AB}) \quad (20)$$

Substituting the value of I_{dc} in Equation (15),

$$\frac{dV_{dc}}{d_t} = \frac{-1}{C_S}\left(\frac{3}{2} K_{CS} \cos\theta_S i_{BC} + \frac{3}{2} K_{CS} \sin\theta_S i_{AB} + \frac{V_{dc}}{R_G}\right) \quad (21)$$

Also, substituting the values of V_{BC} and V_{AB} from Equations (17) and (18) into Equation (14),

$$\begin{bmatrix} i_{BC} \\ i_{AB} \end{bmatrix} = \begin{bmatrix} \frac{-R_S}{L_S} & -W_0 \\ -W_0 & \frac{-R_S}{L_S} \end{bmatrix} \begin{bmatrix} i_{BC} \\ i_{AB} \end{bmatrix} + \frac{1}{L_S} \begin{bmatrix} K_{CS} v_{dc} \cos\theta_S - e_{BC} \\ K_{CS} v_{dc} \sin\theta_S - e_{AB} \end{bmatrix} \quad (22)$$

From Equations (21) and (22), the state-space model for the STATCOM circuit in Figure 1 can be written as follows:

$$\begin{bmatrix} I_{BC} \\ I_{AB} \\ V_{dc} \end{bmatrix} = \begin{bmatrix} \frac{-R_S}{L_S} & W_0 & \frac{1.5K_{CS}\cos\theta_s}{L_S} \\ -W_0 & \frac{-R_S}{L_S} & \frac{1.5K_{CS}\sin\theta_s}{L_S} \\ \frac{1.5K_{CS}\cos\theta_s}{C_S} & \frac{1.5K_{CS}\cos\theta_s}{C_S} & \frac{1}{R_G C_S} \end{bmatrix} \begin{bmatrix} i_{BC} \\ i_{AB} \\ v_{dc} \end{bmatrix} + \begin{bmatrix} \frac{-1}{L_S} & 0 \\ 0 & \frac{-1}{L_S} \\ 0 & 0 \end{bmatrix} \begin{bmatrix} e_{BC} \\ e_{AB} \end{bmatrix} \quad (23)$$

$$\dot{x} = Ax + Bu \quad (24)$$

$$\dot{y} = Cx + d \quad (25)$$

Where: $\dot{x}$ is known as state, u is known as input, $\dot{y}$ is known as output, d is known as disturbance,

$$\dot{x} = \begin{bmatrix} I_{BC} \\ I_{AB} \\ V_{dc} \end{bmatrix} = Ax + Bu \quad (26a)$$

$$x = \begin{bmatrix} i_{BC} \\ i_{AB} \\ v_{dc} \end{bmatrix} \quad (26b)$$

$$A = \begin{bmatrix} \frac{-R_S}{L_S} & W_0 & \frac{K_{GS}\cos\theta_S}{L_S} \\ W_0 & \frac{-R_S}{L_S} & \frac{K_{GS}\sin\theta_S}{L_S} \\ \frac{1.5K_{GS}\cos\theta_S}{C_S} & \frac{1.5K_{GS}\sin\theta_S}{C_S} & \frac{1}{R_G C_S} \end{bmatrix} \quad (27)$$

$$B = \begin{bmatrix} \frac{-1}{L_S} & 0 \\ 0 & \frac{-1}{L_S} \\ 0 & 0 \end{bmatrix} \quad (28)$$

$$u = \begin{bmatrix} e_{BC} \\ \\ e_{AB} \end{bmatrix} \quad (29)$$

B. Modelling of state space equation for predictive control

The generic predictive control is described with the following state space equation given below, and its flow diagram representation was also given in Figure (2);

$$x_{k+1} = Ax_k + Bu_k \quad (30)$$

$$y_k = Cx_k + d_k \quad (31)$$

$$y_{k+1} = Cx_{k+1} + d_k \quad (32)$$

$$y_{k+1} = \mathrm{C}Ax_k + \mathrm{C}Bu_k + d_{k+1} \quad (33)$$

Also, the state space model for the generic predictive control is as given in Eqns (35) and (36), thus

$$x_{k+1} = \mathrm{A}x_k + \mathrm{B}u_k \quad (34)$$

$$y_k = \mathrm{C}x_k + \mathrm{D}u_k + d_k \quad (35)$$

Where: x_{k+1} is known as the state, u_{k+1} is known as input, y_{k+1} is known as output, d_{k+1} is known as disturbance, D is known as the output matrix,

$$x_{k+1} = Ax_k + Bu_k = x_{k+1} = Ax_k + Bu_k \quad (36)$$

$$x_{k+2} = Ax_{k+1} + Bu_{k+1} = x_{k+2} = A(Ax_k + Bu_k) + Bu_{k+1} \quad (37a)$$

$$x_{k+2} = A^2 x_k + ABu_k + Bu_{k+1} \quad (37b)$$

$$x_{k+2} = A^2 x_k + ABu_k + Bu_k \quad (37c)$$

The general expression:

$$x_{k+n} = A^n x_k + A^{n-1} Bu_k + A^{n-2} Bu_{k+1} + \cdots + ABu_{k+n-2} + Bu_{k+n-1} \quad (38)$$

System output:

$$y_{k+n} = Cx_{k+n} + d_{k+n};\ d_{k+n} = d_k \quad (39)$$

$$y_{k+n} = CA^n x_k + C(A^{n-1} Bu_k + A^{n-2} Bu_{k+1} + \cdots + ABu_{k+n-2} + ABu_{k+n-1}) + d_k \quad (40)$$

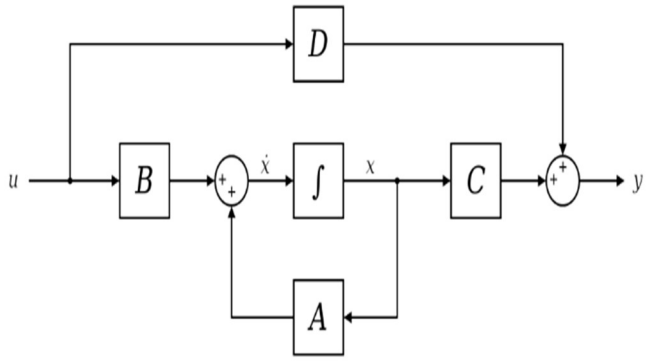

Figure 2: State space representation

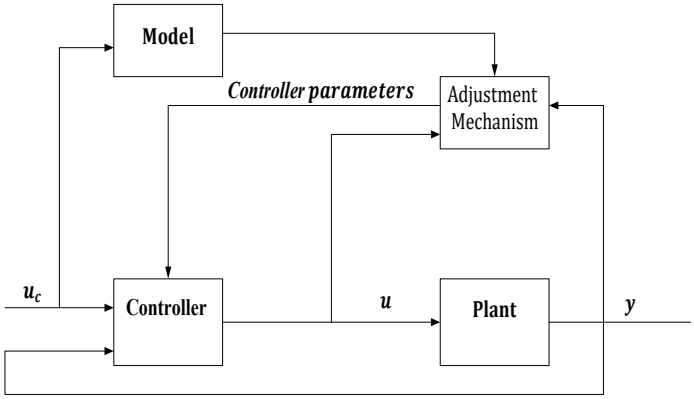

Figure 3. Structure of model reference predictive adaptive controller (Rao and Dash, 2010)

C. Modelling of reference predictive adaptive control

The adaptive servo system is analogous to predictive adaptive control in which the desired response is given as a reference model that initiates the desired response, which triggers a command signal. The MRPAC possesses an ordinary feedback loop (FDL), which comprises the plant, controller, and another FDL that alters the controller parameters based on feedback error. The difference between the plant output (y) and the reference model output is termed the error. Figure 3 depicted the structure of model reference predictive adaptive controller. The parameters can be flexibly adjusted to obtain the loss function for the system, thus

$$J(\theta) = \frac{1}{2}e^2 \quad (41)$$

$$\frac{d\theta}{dt} = -\gamma\frac{\delta J}{\delta\theta} \quad (42)$$

D. Modelling of GA-PID controller

Traditional PID controllers enjoyed industrial applications in the control process due to their exceptional attributes such as simplicity, reliability, and ease of use. This section presents a GA-tuned PID controller, the reference input voltage signal. The synthesis of PID can be described by;

$$u(t) = K_p e(t) + K_I \int_0^t e(t)dt + K_D \frac{de(t)}{dt} \quad (43)$$

Where $e(t)$ = error, $u(t)$ = controller output, K_P = proportionate gain, K_I =Integral gains, and K_D = derivative gains.

F For power quality control of voltage sag, voltage swell, transient, and harmonic, PID parameters were tuned by optimizing an integral absolute error gain by employing genetic algorithm operators, which are selection, reproduction, crossover, and mutation. Table 1 shows the parameters of the GA operators for tuning the PID parameters, while the developed Simulink diagram for GA-PI implementation is presented in Figure 4.

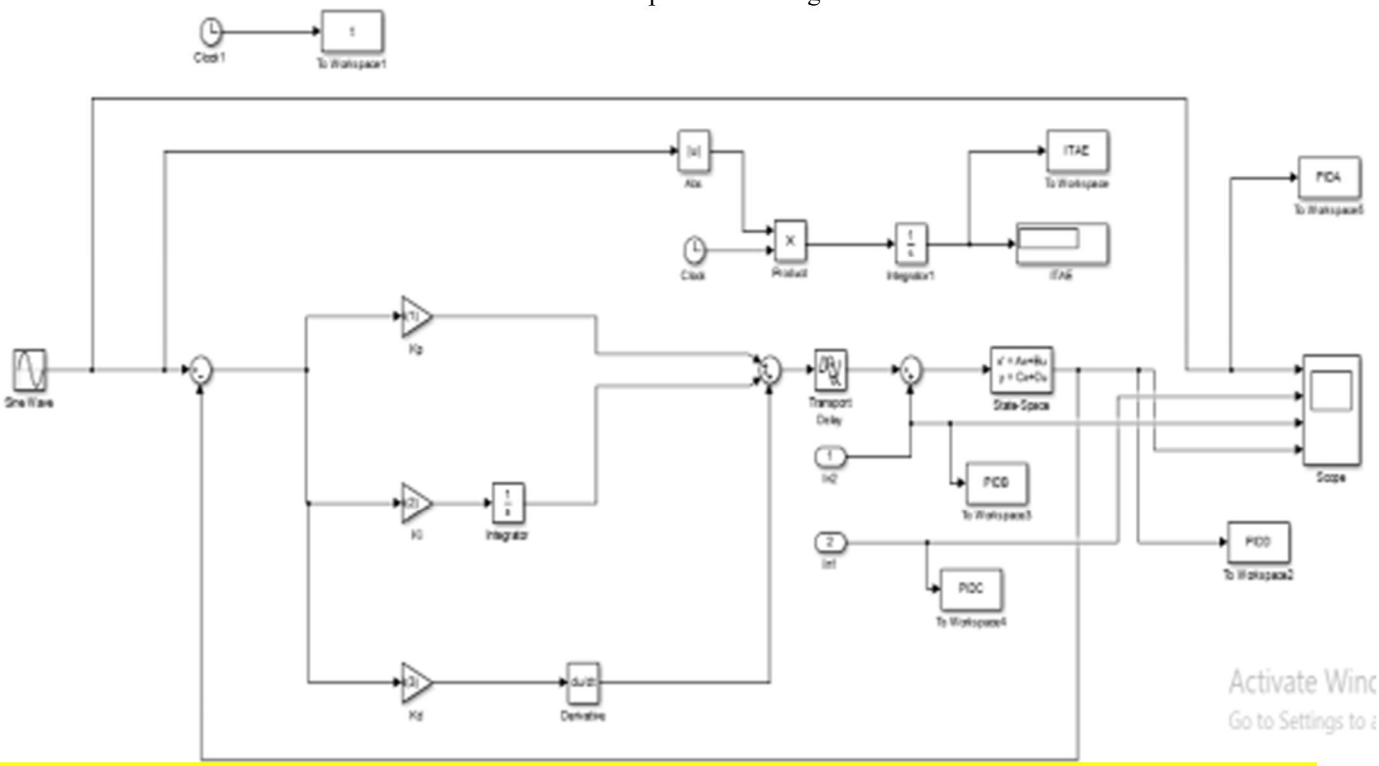

Figure 4: Developed GA-PID Simulink diagram

Table 1: The GA operator's parameters for GA-PID

S/N	Parameters	Specification
1	Number of generations	120
2	Population size	50
3	Mutation probability	0.1
4	Crossover probability	0.2
5	Chromosome length	21

E. Modelling STATCOM control using GA-PI controller

The PI controller exhibits attributes such as reliability in performance and simplicity in function, hence which allows it to be deployed for many of the industrial processes in modern industries. The synthesis of PI can be described by

$$u(t) = K_p e(t) + K_I \int_0^t e(t)dt \quad (44)$$

Where $e(t)$= error, $u(t)$ = controller output, and K_P and K_I = proportional and Integral gains. For power quality control of voltage sag, voltage swell, transient, and harmonic, PI parameters were tuned by optimizing an integral absolute error gain using GA. The GA optimization process is based on the principles of natural genetics, which entail reproduction, crossover, mutation, and natural selection, which are employed for the exploration and exploitation of the search space. The developed Simulink diagram for GA-PI implementation is shown in Figure 5, while the GA parameters used for tuning PI parameters are shown in Table 2.

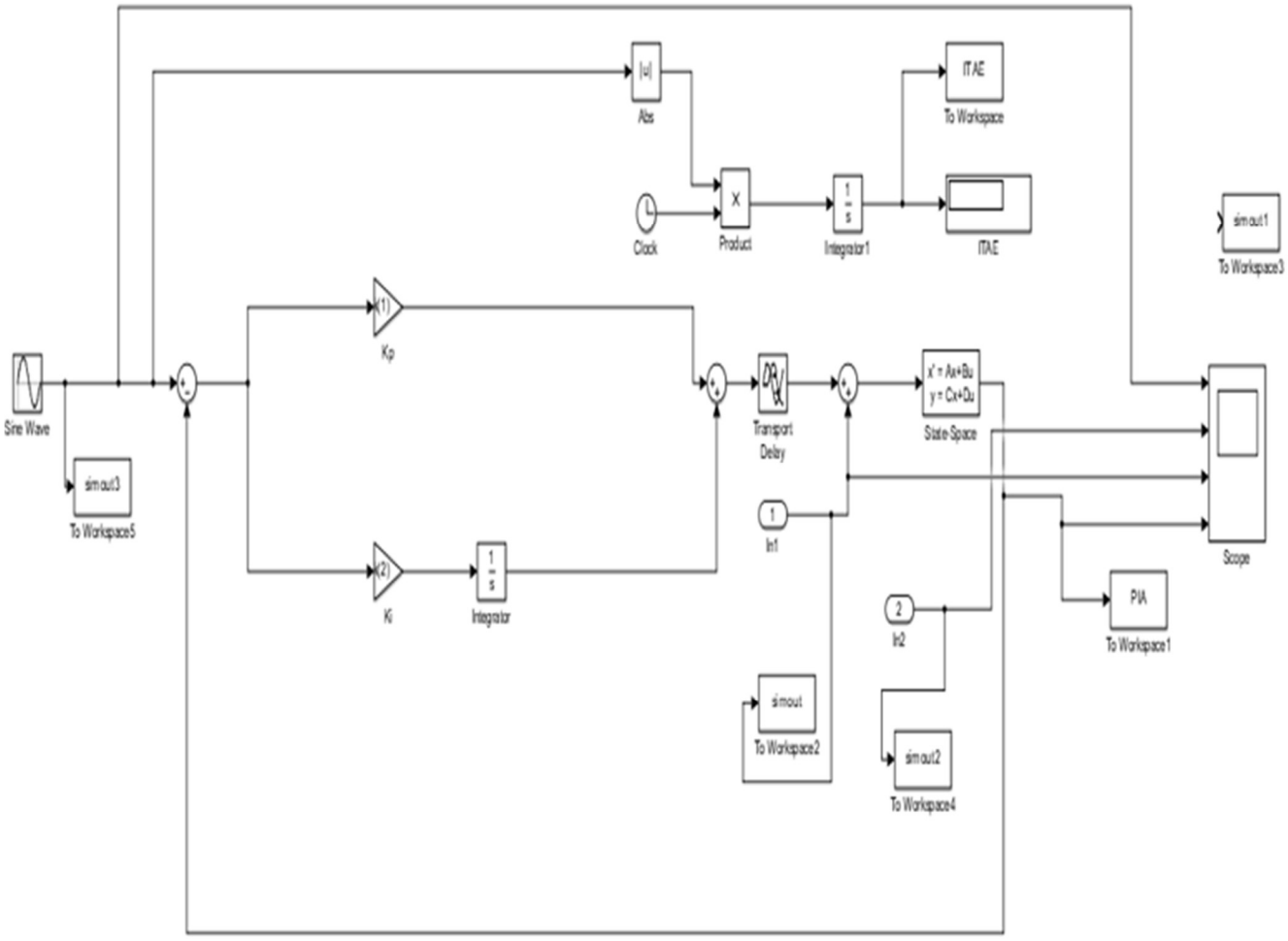

Figure 5: GA-PI Simulink diagram

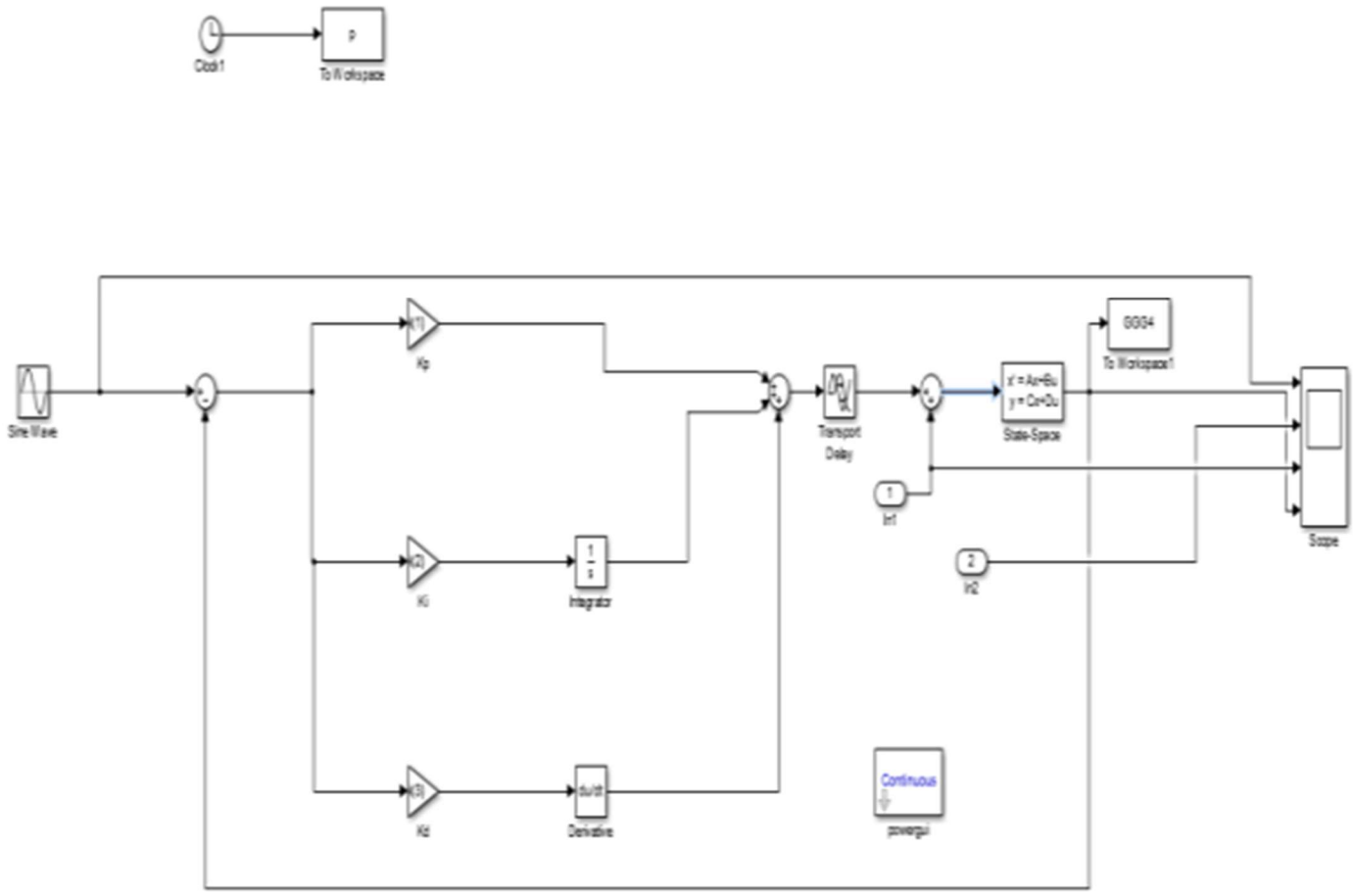

Figure 6: PID Simulink diagram

Table 2: Genetic algorithm operators' parameters for GA-PI

S/N	Parameters	Specifications
1	Number of generations	120
2	Population size	50
3	Mutation probability	0.1
4	Crossover probability	0.2
5	Chromosome length	21

F. Modelling of STATCOM control using a PID controller

Some of the impressive attributes of PID controllers include robust performance, simplicity of functions, performance reliability, minimized steady-state error, faster response, devoid of oscillation, ease of implementation, enhanced system stability, and applicability to linear systems. It is imperative to say that the PID controller uses a generic control loop feedback mechanism to achieve optimum control dynamics (Chauhan *et al.,* 2015). The above-mentioned attributes make them highly suitable for various industrial automation processes in modern industry (Jinghua, 2006). The constituents of PID are Proportional, denoted as (P), Integral, represented by (I), and Derivative, denoted (D). The proportional component is used to achieve the desired set point by adjusting the controller output, the integral is employed to get rid of steady-state error, thereby helping to enhance the system's steady-state performance, and the derivative component helps in improving the system's transient response. The input $e(t)$ and output $u(t)$ are related using Equation (46).

$$U_{(t)} = K_p e(t) + K_i \int_0^t e(t)dt + K_d \frac{de(t)}{dt} \quad (45)$$

Where; $e(t)$= tracking error between the set point and plant output.

The system tracking error designated with variable $e(t)$ connotes the difference between the desired input and the actual output values. Similarly, Figure 6 represents the Simulink diagram developed for PID control implementation.

G. Power acceptability curve

The quantification of the magnitude of bus voltage due to disturbance relative to the duration of disturbance occurrences is termed the power acceptability curve. The original developer of this power acceptability curve is the Computer Business Equipment Manufacturers Association (CBEMA). It is employed to set limits regarding the magnitude and duration of the voltage disturbance so that equipment is not adversely affected. Shown in Figure 6 is the CBEMA curve, and over time, it has been deployed as a standard to measure power system performance. A closer look at Figure 7 showed that there are two conspicuous traces, with the upper layer denoting overvoltage and the lower layer denoting undervoltage, while the region between both the upper trace and lower trace is referred to as the acceptable range.

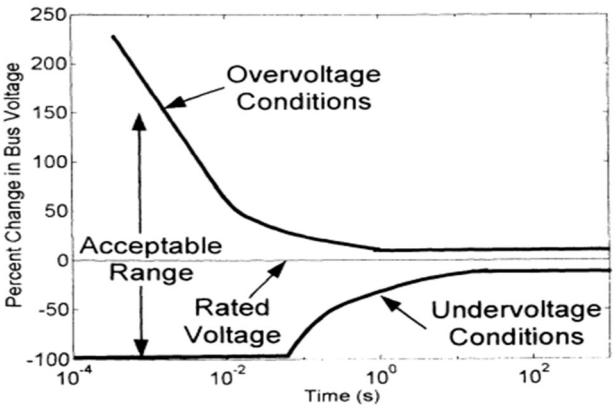

Figure 7: CBEMA curve

III. RESULTS AND DISCUSSION

A. Simulation results on system harmonics

Using the sinusoidal voltage equation expression, the voltage was varied for 250 Hz, 500 kHz, and 700 kHz at the maximum value of 1 p.u from 40 s to 95 s duration to produce a harmonic signal. This harmonic signal served as a disturbance input signal to the MRPAC, GA-PID, GA-PI, and PID controllers. The results obtained for rise time, settling time, and percentage overshoot for MRPAC, GA-PID, GA-PI, and PID for harmonic distortion for MRPAC, GA-PID, GA-PI, and PID for transient from 40 s to 95 s were 0.01%, 10%, 12%, 10%, and 2.5% respectively. To evaluate the performance of the system, a series of measurements has been accomplished. The performance results of MRPAC, GA-PID, GA-PI, and PID for harmonic signals are shown in Table 3.

Table 3: Performance results of MRPAC, GA-PID, GA-PI, and PID for harmonic from 40 s to 95 s

S/N	Controllers	(%) THD
1	MRPAC	0.01
2	GA-PID	10
3	GA-PI	12
4	PID	10
5	IEEE 519	2.5

The performance results of MRPAC, GA-PID, GA-PI, and PID controllers of STATCOM were plotted in Figures 8 to 15, respectively. Total harmonic distortion (THD) was considered against IEEE 519 standards, respectively, for validation, as shown in Figure 6.

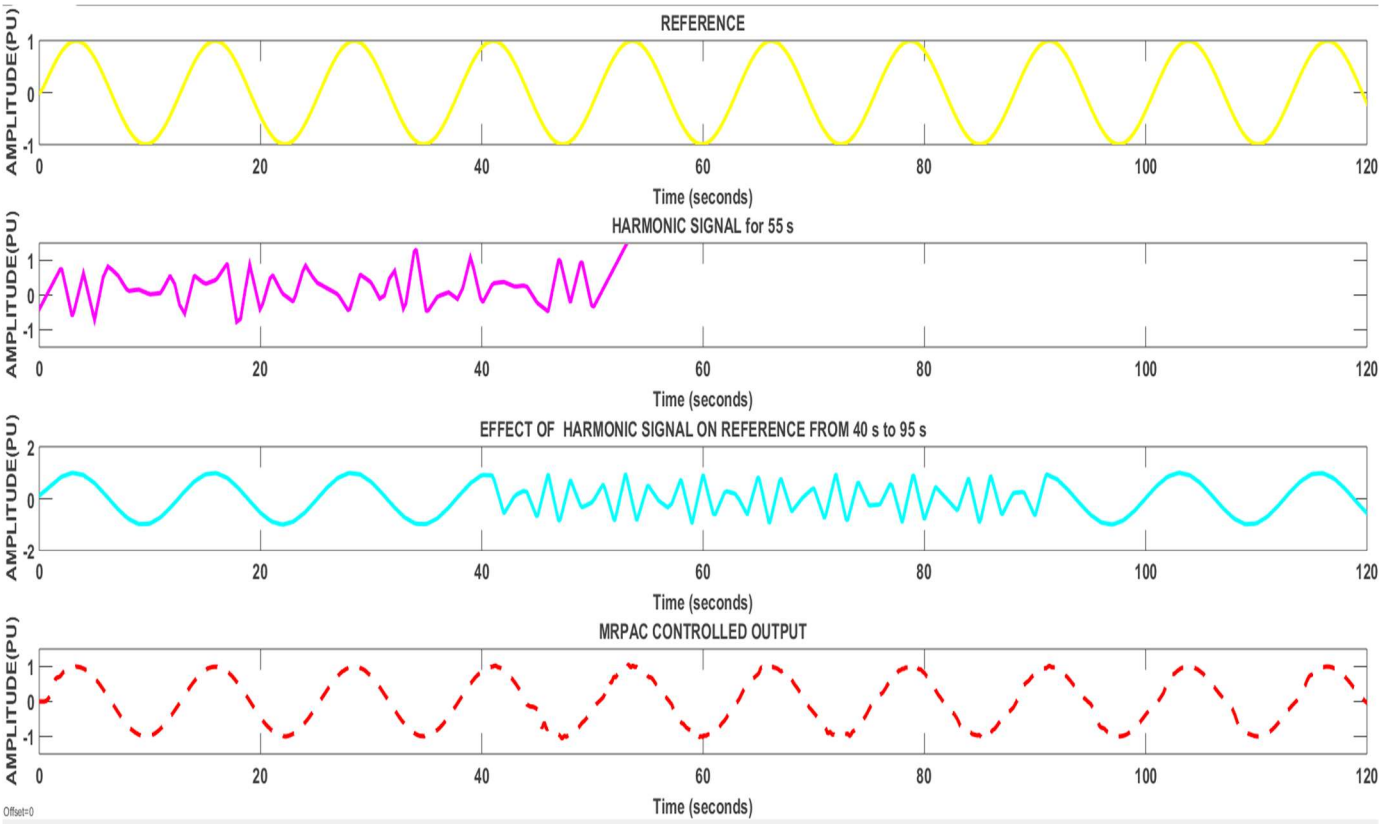

Figure 8: MRPAC output for harmonic from 40 s to 95s

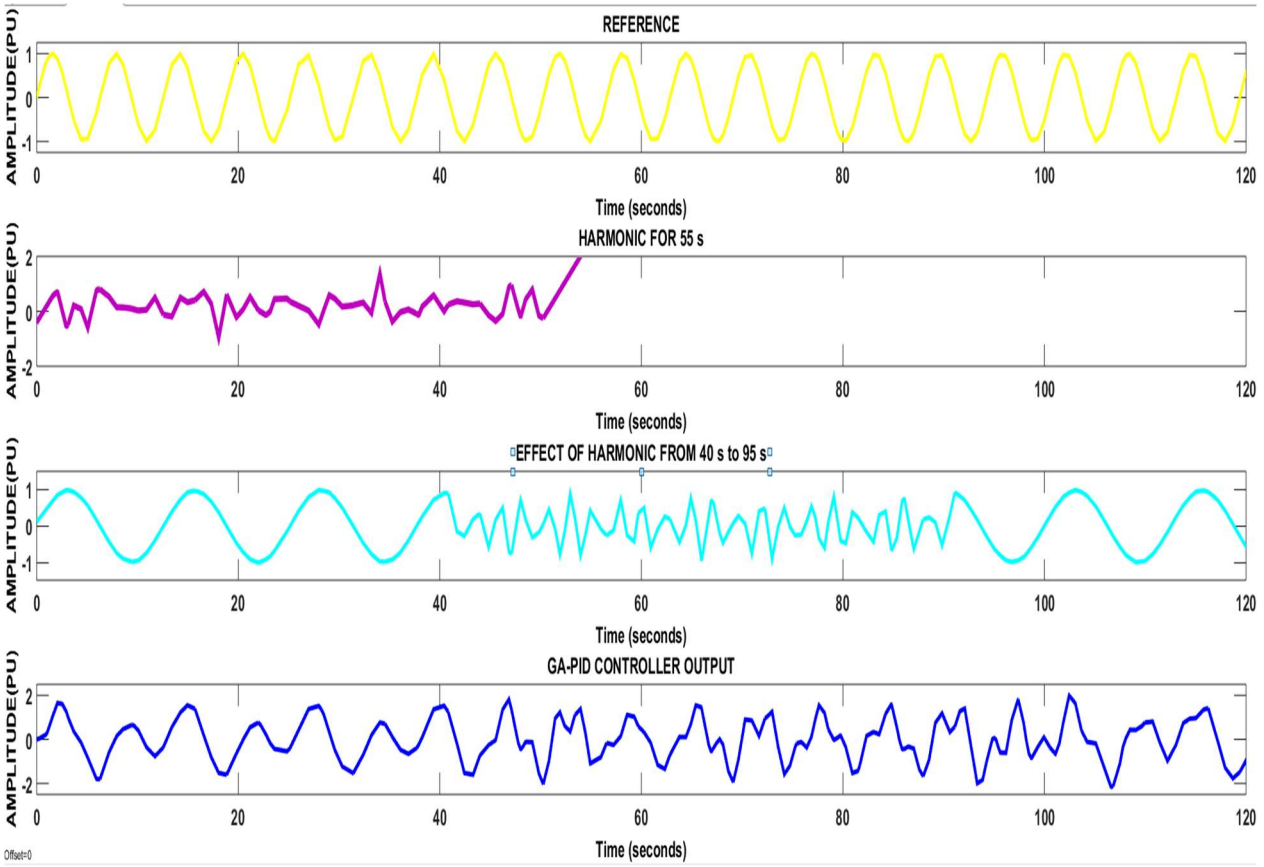

Figure 9: GA-PID output for harmonic from 40 s to 95s

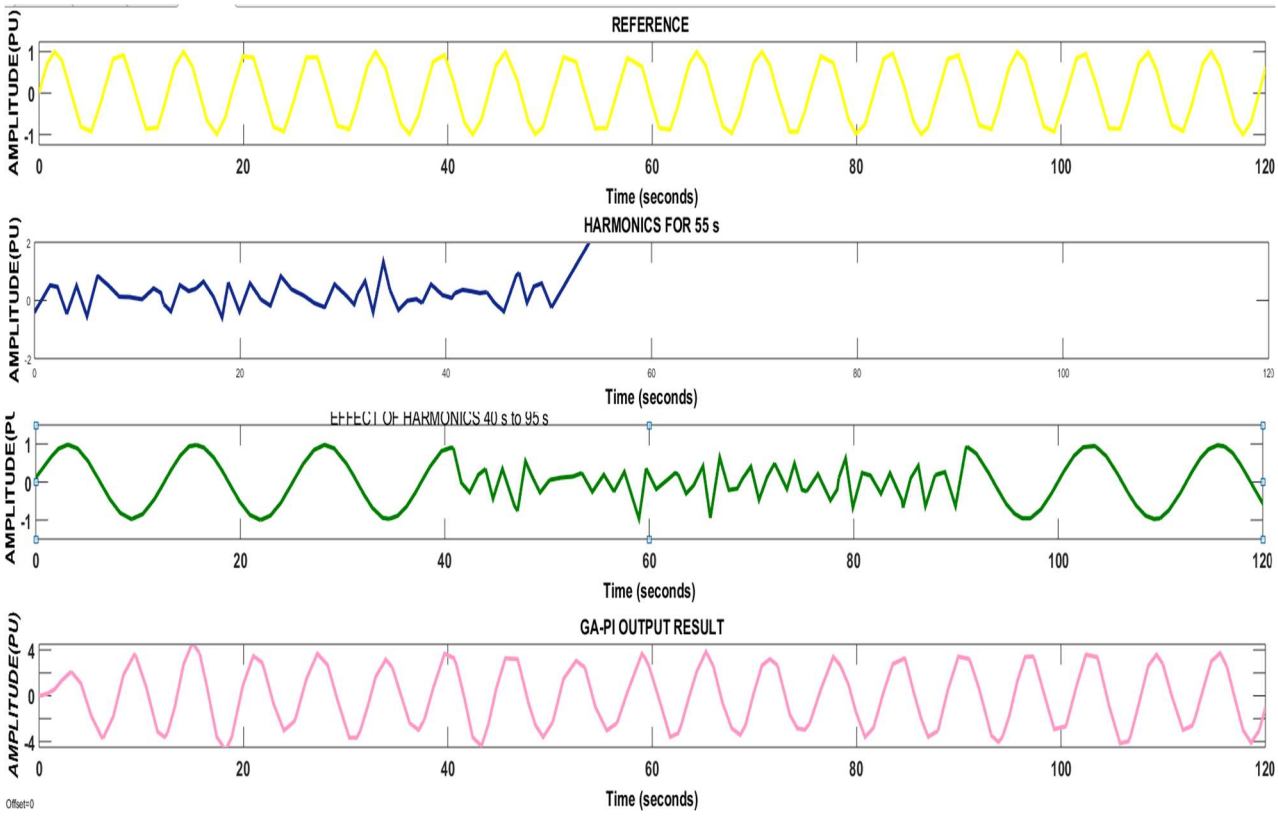

Figure 10: GA-PI output for harmonic from 40 s to 95s

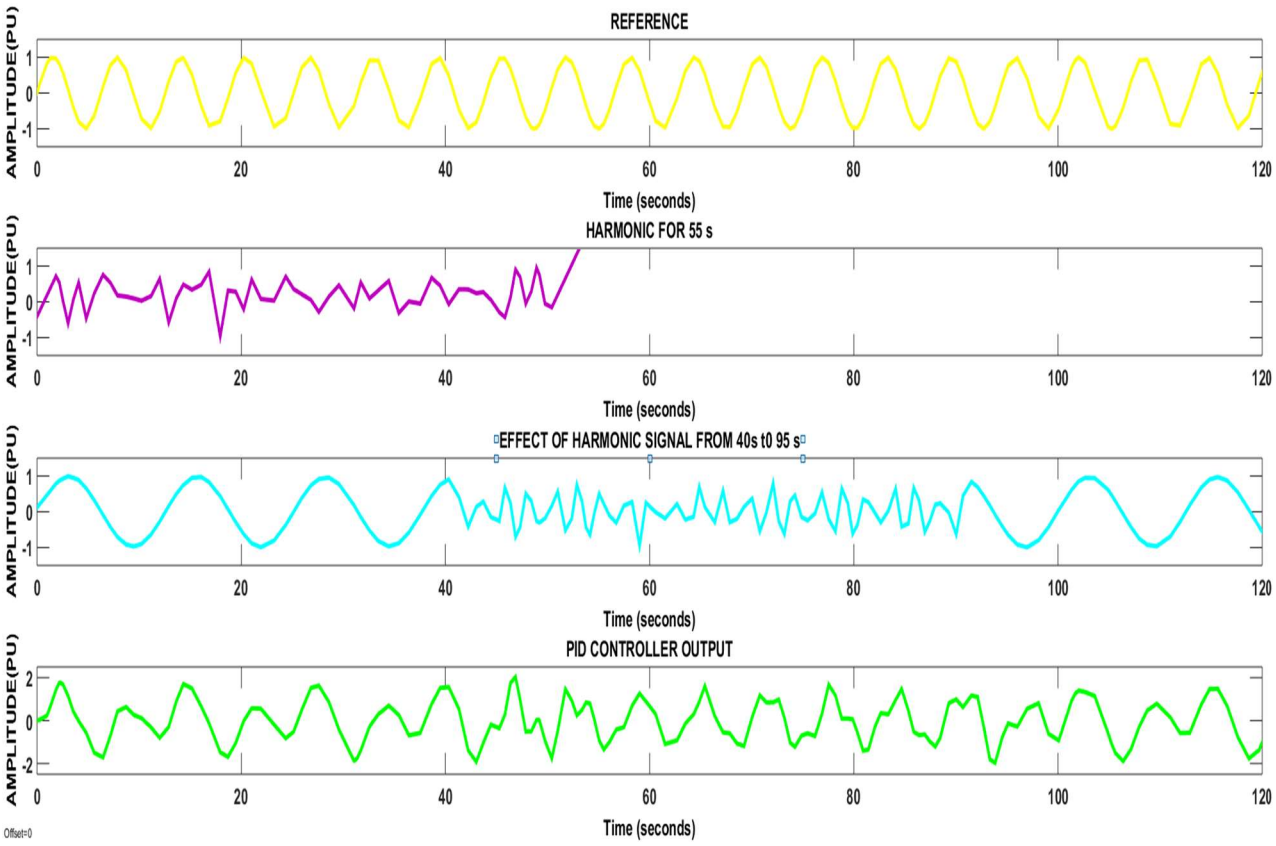

Figure 11: PID output for harmonic from 40 s to 95 s

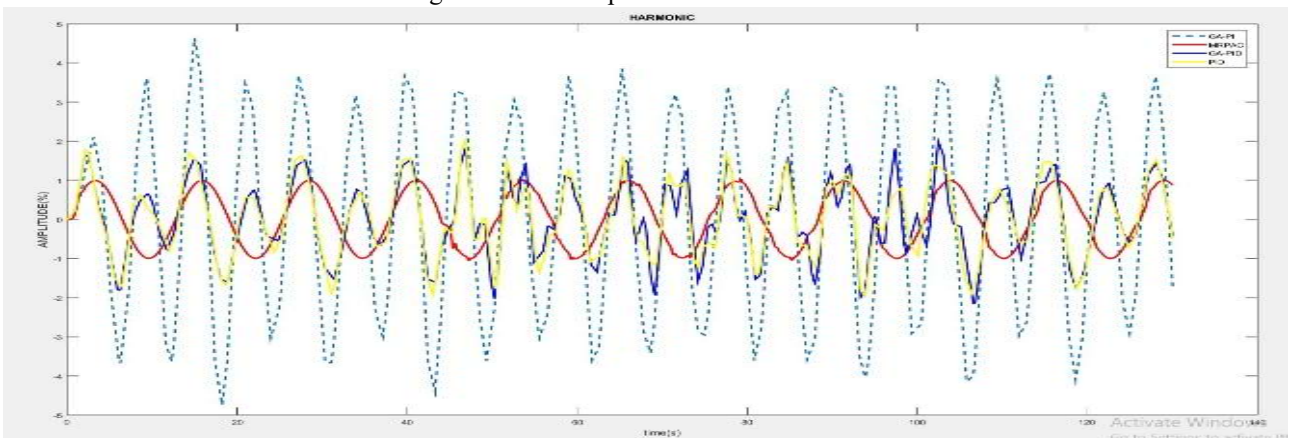

Figure 12: Comparative performance of GA-PI, MRPAC, GA-PID and PID output for harmonic from 40 s to 95s

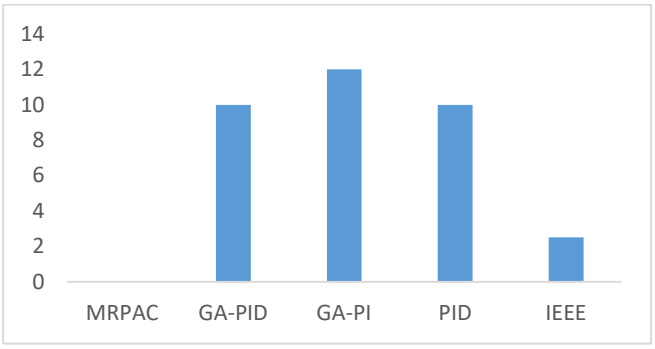

Figure 13: Total harmonic distortion-THD (%) value from 40 s to 95 s for MRPAC, GA-PID, GA-PI, PID, and IEEE

The performance evaluation of the four controllers' study in this research was investigated on the mitigation of voltage sag for a real-time voltage waveform generated between 40 to 80 seconds. Of all the four controllers investigated, MRPAC recorded the least value of rise time, settling time, and percentage overshoot with values of 7s, 0.0001s, and 0.002 % respectively. The least values recorded showed that MRPAC performed better than the rest controllers. The output waveform from the voltage sag from 40 s to 80 s for the four controllers is as shown in Figure 14, while the corresponding performance comparison is presented in Table 4.

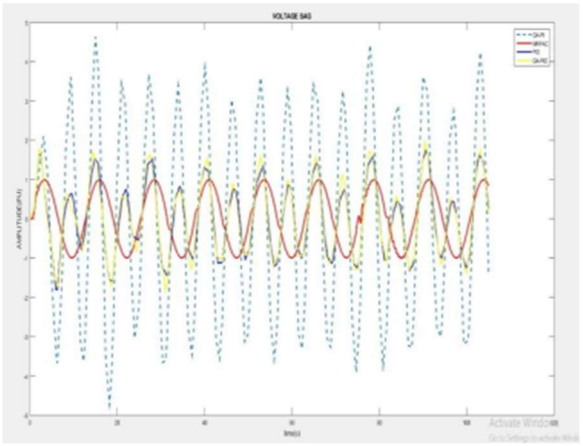

Figure 14. Comparison of GA-PI, MRPAC, PID & GA-PID outputs for voltage sag from 40 s to 80 s

Table 4: Performance results of MRPAC, GA-PID, GAPI, and PID for voltage sag from 40 s to 80 s

S/N	Evaluation metrics	MRPAC	GA-PID	GA-PI	PID	CBEMA
1	RT (s)	7	6.7	8.2	6.7	-
2	ST (s)	0.001	40	100	40	≤ 60
3	% Overshoot	0.002	100	480	200	≤ 10

Also, Table 5 presents the performance comparison of the controllers investigated on the voltage swell on the real-time signal generated between 40 s to 80 s. Just like the case of voltage sag, MRPAC recorded the least value of rise time, settling time, and percentage overshoot, which were estimated to be 7 s, 0.001 s, and 0.002 % respectively. This implies that MRPAC performed better than the rest controllers investigated. The output waveform from the voltage sag from 40 s to 80 s for the four controllers is as shown in Figure 15.

Table 5: Performance results of MRPAC, GA-PID, GAPI, and PID for voltage swell from 40 s to 80 s

S/N	Evaluation metrics	MRPAC	GA-PID	GA-PI	PID	CBEMA
1	Rise time (s)	7	8.4	18	8.9	-
2	Settling time (s)	0.001	90	100	210	≤ 60
3	% Overshoot	0.001	180	470	200	≤ 10

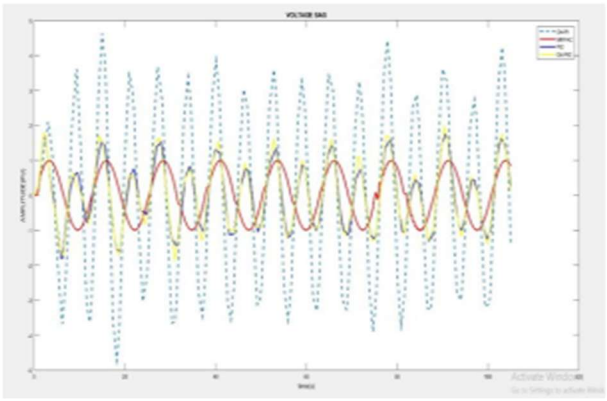

Figure 15: Comparative performance of GA-PI, MRPAC, PID & GA-PID outputs for voltage sag from 40 s to 80

IV. CONCLUSION

This paper presented a comparative performance evaluation of four different controllers for the mitigation of power quality issues such as total harmonic distortion, voltage swell, and voltage sag on a typical 132 kV sub-transmission line. The state space equations for a three-phase STATCOM using differential equations were employed and modelled in a Simulink environment to investigate the performance of MRPAC, GA-PID, GA-PI, and PID control techniques. The comparative analysis revealed that the MRPAC demonstrated a superior performance compared with other controllers, recording the lowest value of rise time, settling time, and overshoot. The validation of MRPAC with the IEEE 519 standard showed that MRPAC performed satisfactorily.

AUTHOR CONTRIBUTIONS

M. O. Okelola: Conceptualization, Methodology. **D.O. Aborisade:** Supervision, **O.Onmoke**: Software, Validation, Writing – original draft, Writing – review & editing. **O.E. Olabode:** Writing – original draft, Writing – review & editing.

REFERENCES

Ajenikoko, G.A & Olabode, O.E. (2017). Optimal power flow with reactive power compensation for cost and loss minimization on Nigerian power grid system. *Indonesian*

Journal of Electrical Engineering and Informatics, 5(3),236-247

Alajrash, B.H., Salem, M, Swadi M, Senjyu, T., Kamarol, M., & Motahhir, S.(2024). A comprehensive review of FACTS devices in modern power systems: Addressing power quality, optimal placement, and stability with renewable energy penetration. *Energy Report*, 11: 5350-5371

Alsammak, A.N., & Mohammed, H.A. (2021). Power quality improvement using fuzzy logic controller based unified power flow controller (UPFC). *Indonesian Journal of Electrical Engineering and Computer Science,* 21(1):1-9

Arikan, O., Kocatepe, C., Ucar, G., Hacialiefendioglu, Y. (2015). Influence of harmonics on medium voltage distribution system: a case study for residential area. *International Journal of Electrical and Computer Engineering,* 9(8): 812-816.

Chauhan R. K., Rajpurohit B. S., Hebner H. E., Singh S. N., & Longatt F. M. G.(2019). Design and analysis of PID and Fuzzy-PID controller for voltage control of dc microgrid. *2015 IEEE Innovative Smart Grid Technologies - Asia (ISGT ASIA)*, Bangkok, Thailand, 2015, pp. 1-6

Ajenikoko, G.A and Olabode, O.E(2017). Optimal power flow with reactive power compensation for cost and loss minimization on Nigerian power grid system. Indonesian Journal of Electrical Engineering and Informatics, 5(3): 236-247

Dekhandji, F.Z., Recioui, A., Ladada, A., & Brahim, T.S.M (2023). Detection and classification of power quality disturbances using LSTM. *Engineering Proceedings,* 29(1):2

Gupta, G., Rai, N.K., & Kumar, D. (2020). Mitigation techniques of power quality issues in electrical power system. *International Research Journal of Engineering and Technology,* 7(1): 974- 979

He, H., & Wang, L. (2022). An identification method of power quality disturbances using kalman filter and extreme learning machine. In Proceedings of the IEEE 5th Advanced Information Management, Communicates, Electronic and Automation Control Conference IEEE, December 2022

Hingoranl N. G., & Gyugyi L. (2000). Understanding FACTS concepts and technology of flexible ac transmission systems. *Wiley Inter Science, John Wiley & sons, inc., publication*, 1-99.

Jinghua, Z (2006). PID controller a short tutorial. Mechanical Engineering, Purdue University, spring, 2006

Johnson, D.O., & Hassan, K.A.(2015). Issues of power quality in electrical systems. *International Journal of Energy and Power Engineering,* 5(4): 148-154

Khetarpal, P., & Tripathi, M.M. (2020). A critical and comprehensive review on power quality disturbance detection and classification. Sustainable Computing: *Informatics and Systems,* 28: 100417

Liang, W.C., Tapan, K.S., & Zhao, Y.D. (2002). Power quality investigation with wavelet techniques. *IEEE Transactions on Power Delivery,* 2(11):28-33

Liao, H., & Milanović, J.V. (2020). On capability of different FACTS devices to mitigate a range of power quality phenomena. *IET Generation Transmission and Distribution*, 1202-1211

Montalvo, J.L., Alfaro-Bernardino, A., Silva, J.C., & Zamora, A. (2024). Power quality events detection, identification, and classification based on the HHDWT hybrid method. *2024 IEEE PES Generation, Transmission and Distribution Latin America Conference and Industrial Exposition (GTDLA)*, Ixtapa, Mexico, 2024, pp. 1-6

Mughal, S., Sharma, N., & Kishore, P.(2022). An analysis of power quality problems and its mitigation. (Accessed 5th May, 2025)

Okelola, M., & Olabode, E (2018). *Application of genetic algorithm solution approach to voltage drop Issues on 33 kV/11 kV injection feeders: a case study of Ogbomoso, South West, Nigeria. Current Journal of Applied Science and Technology,* 27 (4). pp. 1-10.

Okelola, M.O., & Ajenikoko, G.A(2018). Investigation of total harmonic distortion; a case study of some office equipment. *International Journal of Advanced Scientific and Technical Research*, 17-23

Okelola, M.O., & Olabode, O.E. (2018). Application of root mean square and adaptive neuro-fuzzy inference system for power quality events classification using electrical and electronics home appliances as case study. *IOSR Journal of Electrical and Electronics Engineering*, 13(3): 15-23

Okelola, M.O. (2015). Detection and classification of power quality event using discrete wavelet transform and support vector machine. *International Journal of Engineering Research & Technology*,4(6): 338- 342

Okelola, M.O. (2018). Power quality events classification on real-time voltage waveform using short time fourier transform and bayes classifier. *International Journal of Applied Science and Technology*, 8(2): 82-90

Okelola, M.O., Amoo, A.L., & Soremekun, R.K (2019). Power quality events segmentation in a voltage waveform using joint triggering point detection scheme. *FUOYE Journal of Engineering and Technology*, 4(1):8-12

Okelola, M.O., Komolafe, O.A., & Aborisade, D. O. (2015). Improving the detection of power quality events in real – time electrical voltage. *International Journal of Scientific and Engineering Research*, 6(8), 400 – 404

Olabode O.E., Oni D.I, & Obanisola O.O.(2017). An overview of mathematical steady-state modelling of newton-raphson load flow equations incorporating ltct, shunt capacitor and facts devices. *International Journal of Advanced Research in Science, Engineering and Technology,* 4(1): 3163- 3172

Olabode, O.E., Akinyele, D.O, Ajewole, T.O., Omogoye, S.O., & Raji, A.A. (2024). Impact of integrating type-1 distributed generation on distribution network using modified genetic algorithm and voltage stability index: a technical and cost–benefit analysis approach. *Journal of Engineering and Applied Science*, 71:222.

Olabode, O.E., Ayantunji, O.D., & Nwagbara, V.U(2017). Performance evaluation of reactive power compensation of TCSC and SVC on voltage profile enhancement and power system loss minimization. *International Journal of Scientific & Engineering Research*, 8(8): 1514- 1519.

Olotuah, H.G., Oyetunji, S.A., Olabode, O. E., Asolo, S.O., Adeleke, A.A., & Ijawoye, R.O. (2025). Effect of varying base transceiver station parameters on the power

density distribution in Southwestern Nigeria using Cost-231 Hata model. *Journal of Engineering, Innovation and Sustainability,* 1(1): 35 - 49

Pilawa-Podgurski, R (2020). The future of power electronics circuits: new technologies and managed complexity will drive the future. *IEEE Power Electronics Magazine,* 7(2):41-43.

Prasad, H., & Sudhakar, T. D.(2015). Design of active filters to reduce harmonics for power qualify improvement. *2015 International Conference on Computation of Power, Energy, Information and communication, 3*36-344

Rao, R.V.D., & Dash, S.S. (2021). Enhancement of power quality by using unified power quality conditioner with pid and fuzzy logic controller. *International Journal of Computer Applications*,5(7): 21- 27.

Rao, R.V.D.R., & Dash, S.S.(2010). Enhancement of power quality by using unified power quality conditioner with PID and fuzzy logic controller. *International Journal of Computer Applications*, 5(7):21-27

Singh, R., Arun Pachori, A., & Pandey, P.K. (2021). Pid controller-based power quality improvement using statcom. *Webology*, 18(4): 1703- 1711

Su, H., Luo, Z.A., Feng, Y.Y., & Liu, Z.S.(2019). Application of siemens plc in thermal simulator control system. *Procedia Manufacturing,* 37: 38–45

Xi, Y., & L, X. (2023). Classification of multiple power quality distrbances based on continuous wavelet transform and lightweight convolutional neural network. *Energy Science and Engineering*, 1–18

Yao, K, Lin C., & Pan, C. (2024). Industrial sustainable development: the development trend of programmable logic controller technology. *Sustainability*, *16*(14): 6230